

On photonic controlled phase gates

K. Kieling¹, J. O’Brien², and J. Eisert^{1,3}

¹*Institute of Physics and Astronomy, University of Potsdam, 14476 Potsdam, Germany*

²*Centre for Quantum Photonics, H. H. Wills Physics Laboratory and Department of Electrical and Electronic Engineering, University of Bristol, Bristol BS8 1UB, UK and*

³*Institute for Advanced Study Berlin, 14193 Berlin, Germany*

(Dated: November 3, 2018)

As primitives for entanglement generation, controlled phase gates take a central role in quantum computing. Especially in ideas realizing instances of quantum computation in linear optical gate arrays a closer look can be rewarding. In such architectures, all effective non-linearities are induced by measurements: Hence the probability of success is a crucial parameter of such quantum gates. In this note, we discuss this question for controlled phase gates that implement an arbitrary phase with one and two control qubits. Within the class of post-selected gates in dual-rail encoding with vacuum ancillas we identify the optimal success probabilities. We construct networks that allow for an implementation by means of today’s experimental capabilities in detail. The methods employed here appear specifically useful with the advent of integrated linear optical circuits, providing stable interferometers on monolithic structures.

PACS numbers: 03.67.Lx, 42.50.Ex, 42.50.Dv

I. INTRODUCTION

Linear optical architectures offer the potential for reliable realizations of small-scale quantum computing [1]. In the recent past, numerous proof-of-principle demonstrations have relied on the precise state manipulation that is available using linear optical elements. The development of better and brighter sources with good mode quality as well as new types of detectors have opened up new perspectives [2] in state preparation and manipulation, for six or more photons. Specifically, integrated optical circuits allow for state manipulation with little mode matching problems in interferometers [3].

Naturally, significant efforts have been devoted towards realizing instances of quantum gates. As primitives for such small-scale computing, two-partite quantum gates delivering a controlled phase-shift of φ have already been experimentally demonstrated (see Refs. [4–6] for $\varphi = \pi$ and Ref. [7] for general phases). In this note, we focus on linear optical implementations of phase gates with arbitrary phases. In particular, we will ask when arbitrary phases can be realised in the first place, and—one of the main figures of merit in linear optical applications—what the optimum probabilities of success are, as any non-linear map is necessarily probabilistic. A realisation of such gates seems interesting from the perspective of

- (i) gaining an understanding of the probabilistic character of quantum gates as well as
- (ii) serving as a proof of principle realisation of a kind of quantum gate that has several applications in linear optical quantum information processing.

As far as the first aspect is concerned, one may well expect that there is a trade-off between the notorious problem of having a small probability of success and the phase that is being realised in the gate. In fact, the study in Ref. [8] suggests exactly such a behavior: the presented upper bounds to the probability of success increase from the minimum at

$p_s(\varphi = \pi) = 1/4$ to $p_s(0) = 1$. To investigate such a trade-off is interesting in its own right and helps in building intuition concerning the probabilistic behavior of linear optics. One may well develop the intuition that “large phases are costly” as far as the probability of success and hence the overhead or repetition are concerned.

Further, concerning the second aspect, there are several applications for which such a trade-off is relevant. In linear optical architectures, it may be a good idea to have a smaller phase, if one only has higher success probabilities. The new measurement-based quantum computational models [9] for example offer this perspective: One does not have to have controlled π phase gates to prepare cluster states, but one would in principle also get away with smaller phases. This may well (but does not have to be) a significant advantage when preparing resources for measurement-based quantum computing different from cluster states [9, 10].

Of course, in standard gate-based quantum computing, one will typically encounter all kinds of controlled phase gates. For example, in the quantum Fourier transform [11], one has to implement several controlled phase gates. They can again be decomposed into other sets of universal gates (like CNOT or CZ and local unitaries). But, in terms of resource requirements, it is obviously an advantage to directly implement the relevant quantum gates with phases in the range $0 < \varphi < \pi$. There are also interesting trade-offs between resource requirements and success probabilities in a number of related contexts, like non-local gates in distributed quantum computation [12, 13]. Refs. [13], for example, study distributed controlled phase-gates which would need less entanglement and succeed with a higher probability. In the field of linear optics gates, numerical results on direct implementation of arbitrary two-qubit gates are known (see Ref. [14] and references therein).

Instead of resorting to decompositions in the circuit model, one could gain from implementing unitaries in a fashion “natural” to the respective architecture at hand. In the case of linear optics it means to leave the computational sub-space

given by the encoding of the qubits for the sake of taking a “shortcut” through higher dimensions [7]. Given that the fundamental information carriers are implemented using bosonic modes, this will occur when mixing those modes in beam splitter networks and is an inherent feature of genuine linear optics implementations, in contrast to decompositions into standard gate sets.

Here we will study post-selected gates, so not genuine “event-ready” quantum gates, but—as is common in linear optical architectures at least to date—those where one measures the output modes and whether the gate actually succeeded is determined only *a posteriori* by accepting only those outcomes which lie in the computational dual-rail subspace of the Hilbert space of n photons on $2n$ modes. Incorporating less constraints, these gates concern only a smaller number of modes and are still within reach of current experiments. In principle non-demolition measurements of the output would be required for an event-ready gate.

II. CONTROLLED PHASE GATES

A. Single beam splitter

In a post-selected phase gate on four modes in the standard dual-rail encoding, two of the modes are merely involved as “by-standers”, in that their amplitude is compensated in exactly the same fashion as in Refs. [4–6]. In this section, we will hence concentrate on two modes forming the “core” of the scheme, giving rise to a two-qubit dual-rail phase gate on four physical modes. The core itself may be regarded as a single-rail phase gate in its own right. Later we will see that not breaking the network into a core and by-stander modes will not give any advantage.

Similar to Ref. [4] we will briefly investigate the consequences of simply having a single beam splitter forming the core of the quantum gate. The action on the photonic creation operators of the two involved modes it is mixing is described by the matrix

$$U = \text{diag}(e^{i\phi_1}, e^{-i\phi_1}) \cdot B \cdot \text{diag}(e^{i\phi_2}, e^{-i\phi_2}) \quad (1)$$

with

$$B = \begin{bmatrix} \sin(\vartheta) & \cos(\vartheta) \\ -\cos(\vartheta) & \sin(\vartheta) \end{bmatrix} \quad (2)$$

and appropriate phases $\phi_1, \phi_2 \in [0, 2\pi)$ and mixing angle $\vartheta \in [0, 2\pi)$. The phases can also be realised deterministically by local operations on the dual-rail qubits, which leaves the relevant part of the gate $U' = B$. The matrix elements of the unitary U' belonging to U' for vacuum, single photon operation, and the two-photon component read

$$\langle 0, 0 | U' | 0, 0 \rangle = 1, \quad (3)$$

$$\langle 1, 0 | U' | 1, 0 \rangle = A_{1,1} = \sin(\vartheta), \quad (4)$$

$$\langle 0, 1 | U' | 0, 1 \rangle = A_{2,2} = \sin(\vartheta), \quad (5)$$

$$\langle 1, 1 | U' | 1, 1 \rangle = \text{per}(A) = \cos(2\vartheta) = 1 - 2\sin^2 \vartheta, \quad (6)$$

respectively. Since we are restricted to $n \leq 2$ modes, these four quantities determine the action of the core completely. With the constraint

$$1 - 2\sin^2(\vartheta) = \sin^2(\vartheta) \quad (7)$$

that ensures equal single- and two-photon amplitudes (equal probabilities for all dual-rail states), only the two solutions $\vartheta = \pm \arcsin(3^{-1/2})$ are possible, giving rise to $\varphi = 0, \pi$, respectively.

Hence, one finds that in this way, one *can* implement quantum phase gates, but only two different ones: One is not doing anything, and the other ones effect is a controlled phase of π . This is exactly the gate of Refs. [4, 5]. In other words, without invoking at least a single additional mode, one can not go beyond the known π -phase in this fashion.

B. Arbitrary phases

However, we can extend this scheme: The restriction to unitary two-mode beam splitters can be relaxed. Instead of starting with $U \in SU(2)$, we use an arbitrary matrix $A \in \mathbb{C}^{2 \times 2}$. Then we will embed the two-mode matrix into a higher dimensional unitary, such that an appropriately rescaled A forms a principle submatrix of a larger unitary matrix A' . The optimal rescaling is simply dictated by the largest singular value of A . We will see that in the two-mode case only a single additional mode is already the most general extension, so the full set-up would consist of a transformation on three modes involving at most three beam splitters. In this class of gates, for each φ , the one with the optimal probability of success $p_s(\varphi)$ can be identified.

Observation 1 (Optimal post-selected dual-rail controlled phase gate). *Consider linear optics, an arbitrary number of auxiliary vacuum modes and photon number resolving detectors. When post-selecting the state of the signal modes onto the computational sub-space and the auxiliary modes onto the vacuum, the optimal network on four modes implementing the gate represented in the computational basis of two dual-rail qubits by $U = \text{diag}(1, 1, 1, e^{i\varphi})$, $\varphi \in [0, \pi]$, has a success probability (shown in Fig. 1) of*

$$p_s(\varphi) = \left(1 + 2 \left| \sin \frac{\varphi}{2} \right| + 2^{3/2} \sin \frac{\pi - \varphi}{4} \sqrt{\left| \sin \frac{\varphi}{2} \right|} \right)^{-2}. \quad (8)$$

Proof: In order to find p_s —the same for all possible input states—we will first construct the linear transformation of the relevant creation operators and identify the optimal unitary extension afterwards.

- *Two-mode transformation:* The two-mode transformation resulting from solving the equations (3)–(6) imposed by the gate we want to build is

$$A = p_s^{1/4} \begin{bmatrix} x & (e^{i\varphi} - 1)x/y \\ y/x & 1/x \end{bmatrix}. \quad (9)$$

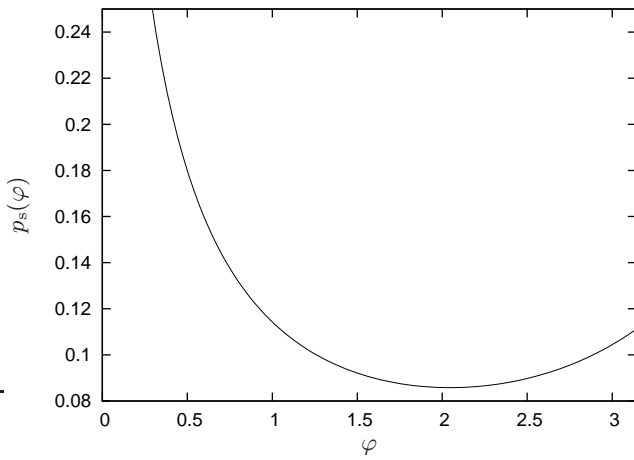


FIG. 1. Optimal success probability $p_s(\varphi)$ of phase gates with vacuum ancillas (one vacuum ancilla is already optimal) vs. the phase φ (solid line). At $\varphi = \pi$ the result of Refs. [4, 5], $p_s(\pi) = 1/9$, is reproduced. The intuitive assumption of a monotonous $p_s(\varphi)$ is not fulfilled: indeed, the success probability is worse than $1/9$ in the interval $\pi/3 < \varphi < \pi$. Due to phases $\varphi < \pi$ not being implementable with a single beam splitter, the additional unitary extension requires further measurements and therefore decreases the probability of success near $\varphi = \pi$.

x and y are free non-zero complex parameters. By writing

$$A = p_s^{1/4} \text{diag}(a, a^{-1}) \cdot \begin{bmatrix} 1 & e^{i\varphi} - 1 \\ 1 & 1 \end{bmatrix} \cdot \text{diag}(b, b^{-1}), \quad (10)$$

with $a = xy^{-1/2}$ and $b = y^{1/2}$ we see that the singular values of A only depend on $|a|^2$ and $|b|^2$, so not on the phases of a, b , and x and y .

The general solution to the dual-rail problem is actually composed of the transformation A together with appropriate damping of the by-standers: the probability of success can not be enhanced by considering a full transformation on all four modes. This can be seen by writing the polynomial system given by the dual-rail problem similar to (3)–(6), consisting of 16 quadratic equations in the matrix elements of $B \in \mathbb{C}^{4 \times 4}$. It turns out that by permuting modes and appropriate variable substitutions all solutions can be brought into the form $B \propto \mathbb{1}_2 \otimes A$, consisting of the two-mode core given in Eqn. (9) and two by-passed modes.

- *Optimal extension:* Given the 2×2 matrix A that realises the transformation we are looking for, the optimal unitary extensions can be identified. Let us extend the first and second row vectors (denoted by A_1 and A_2) to dimension 3 by appending $A_{1,3}$ and $A_{2,3}$, respectively, in such a way as to allow for unitarity of the extended matrix, $A' \in SU(3)$.

To see why a dimension of three is already sufficient consider a linear transformation of the creation operators of n modes, described by its a (not necessarily uni-

tary) matrix A . By using the singular value decomposition (SVD) it can be decomposed as $A = V \cdot D \cdot W^{-1}$ where V and W are unitary (and therefore have immediate interpretations as physical beam splitter matrices themselves), and $D = \{d_1, \dots, d_n\}$ is a diagonal matrix with real non-negative entries $d_1 \geq d_2 \geq \dots \geq d_n$, the singular values. In terms of linear optics D can be interpreted as mixing each mode $k = 1, \dots, n$ with an additional mode $n+k$ in the vacuum state which will be post-selected in the vacuum afterwards [15, 16]. Then, d_k describes the transmittivity of the beam splitter used to couple modes k and n_k . Without loss of generality one can assume $d_1 = 1$, vacuum mixing for the first mode. This can be achieved by rescaling with the inverse of the largest singular value, so $A \mapsto d_1^{-1}A$, which implies $d_k \mapsto d_1^{-1}d_k$. Note that such a “global” rescaling of A does not change the post-selected action on the computational sub-space but only the success probability of it according to $p_s \mapsto d_1^{-2n}p_s$. Therefore, in general, there are $n-1$ additional vacuum modes required to extend an n -mode linear transformation to a unitary, and thus physical, network. Also please note, that the constraint $d_1 = 1$ has to be taken into account for any optimisation of success probabilities of A . Here we will not explicitly use this decomposition further, but the constraint will be implemented implicitly by requiring the $n-1$ -mode extension to be unitary.

In our specific 3-mode extension we choose $A_{1,3}$ and $A_{2,3}$ such that the new row vectors are orthogonal. By multiplying them by the root of the inverse of their respective norms, $|A'_1|$ and $|A'_2|$, they will be normalised. Finding a third orthogonal vector to fill the unitary matrix can be done with the complex cross product $(A'_1 \times A'_2)^*$, or in general by choosing a vector at random and orthogonalising it with respect to the given ones.

The dependence of the success probability on the extension is

$$p_s = (|A'_1||A'_2|)^{-2}. \quad (11)$$

Therefore, the objective is to

$$\text{minimise } f = |A'_1|^2 |A'_2|^2 \quad (12)$$

$$\text{subject to } A'_1(A'_2)^\dagger = A_1 A_2^\dagger + A_{1,3} A_{2,3}^* = 0. \quad (13)$$

The first observation is that the row-scaling by x is already included in the norm of the row vectors, leaving us with one parameter less. By using the phase of y , we can assure that $A_1 A_2^\dagger$ is real and positive and also $\arg(A_{1,3}) - \arg(A_{2,3}) = \pm\pi$. This constrained minimisation problem in $A_{1,2}$ and $A_{1,3}$ can indeed be solved (by using Lagrange’s multiplier rule and showing constraint qualification) and we find $|y| = (2(1 - \cos \varphi))^{1/4}$. Then an optimal solution (phases chosen conveniently) is

$$A_{1,3} = A_{2,3}^* = e^{i\pi/2} \left(\sqrt{2 \left| \sin \frac{\varphi}{2} \right| \sin \frac{\pi - \varphi}{4}} \right)^{1/2} \quad (14)$$

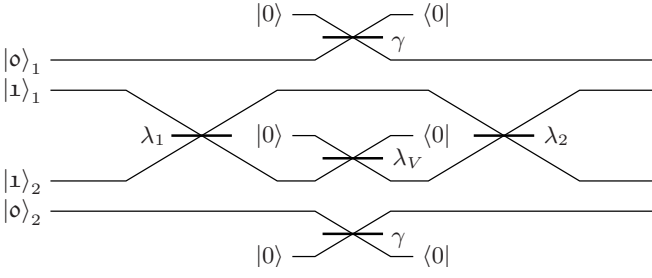


FIG. 2. Basic spatial modes based set-up obtained from translating an arbitrary 2×2 core into the language of linear optics. The core extension is provided by mixing with a vacuum mode on the central beam splitter. This mode, in turn, has to be post-selected in the vacuum state afterwards. The upper and lower beam splitters implement the appropriate compensation by damping the by-passed modes (which is the same for both modes for the optimal solution which we consider).

The labels at the beam splitters will be used to identify them with the respective optical elements in Figs. 3–5. In general, the parameters (i.e., reflectivity and phases) of these elements depend on the gate’s phase φ . Further, the notation $|0\rangle_i$ and $|1\rangle_i$ is used for the logical 0/1-modes of the i -th qubit to avoid confusion with Fock states.

with the probability of success given by

$$p_s(\varphi) = \left(1 + |y|^2 + |y|\sqrt{2 - |y|^2}\right)^{-2} \quad (15)$$

$$= \left(1 + 2 \left|\sin \frac{\varphi}{2}\right| + 2^{3/2} \sin \frac{\pi - \varphi}{4} \sqrt{\left|\sin \frac{\varphi}{2}\right|}\right)^{-2}.$$

The reflectivities of the compensating beam splitters in the by-passed modes have to be chosen such that the success probability is constant for all dual-rail states, i.e.,

$$r = p_s^{1/4}. \quad (16)$$

The success probability $p_s(\varphi)$ of this gate is shown in Fig. 1. Interestingly—and quite surprisingly—the worst success probability is not achieved for the sign-flip ($\varphi = \pi$), but for $\varphi \approx 2.05$. This means, gates delivering a phase shift slightly smaller than π and thereby generating less entanglement will not give rise to a larger, but to a smaller success probability. As expected, the success probability for very small phases increases and reaches unity for $\varphi = 0$: one can always do nothing at all with unit success probability.

C. Integrated quantum photonics realizations

Sophisticated circuits such as the one shown in Fig. 5 can be built from bulk optical elements (mirrors, beamsplitters, etc.) Such circuits often require implementation of Sagnac interferometers (e.g., Ref. [18]), partially polarizing beam splitters (PPBSs) [6], or beam displacers [19, 30] to achieve interferometric stability. For the most complicated circuits a combination of these elements is required. Indeed a (non-optimal)

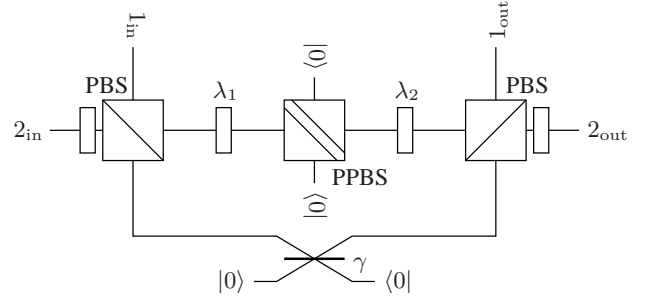


FIG. 3. Setup for a controlled phase gate on two polarisation encoded dual-rail qubits. The logical modes of the two qubits are separated and re-united by means of polarising beam splitters (PBS). Replacing the left and right beam splitters in Fig. 2 by wave plates λ_1 and λ_2 , they become easier to tune to different φ , and provide better stability. The lower beam splitter, γ , implements compensation of both, $|0\rangle_1$ and $|0\rangle_2$, modes. λ_V is taken care of by the partially polarising beam splitter (PPBS, allowing for different reflectivities for the two polarisations, further explained in Fig. 4) in the centre. Additionally, one of the qubits has to be flipped prior to and after the circuit, which here is done by acting with a wave plate on the second qubit.

implementation of a two-qubit controlled unitary gate used a combination of beam displacers and PPBSs [7]. However, such circuits are extremely challenging to align, are limited in performance by the quality of that alignment, and are ultimately not scalable.

An alternative approach based on lithographically fabricated integrated waveguides on a chip has recently been developed [3]. This approach has demonstrated better performance, in terms of alignment and stability, as well as miniaturization and scalability. The monolithic nature of these devices enables interferometers to be fabricated with precise phase and stability, making the Mach-Zehnder interferometer shown in Fig. 2 directly implementable without the need to stabilize the optical phase (either actively, or using the Sagnac-type architecture of Fig. 5), greatly simplifying the task of making complicated circuits: Essentially the circuit one draws on the blackboard can be directly ‘written’ into the circuit. Indeed, integrated photonics circuits have been used to implement a circuit of several logic gates on four photons, to implement a compiled version of Shor’s quantum factoring algorithm in this way [20]. In fact laser direct write techniques have been used to ‘write’ circuits in an even more direct fashion than the lithographic approach.

Another key advantage of integrated quantum photonics for the circuits described here is that on-chip phase control can be directly integrated with the circuit [21], which could allow measurement of the success probability curve (Fig. 1 or Fig. 6 for example) to be directly mapped by sweeping the applied voltage.

D. Experimental issues in free space

In order to render the proposed gates experimentally more feasible in free space, some simplifications have to be done

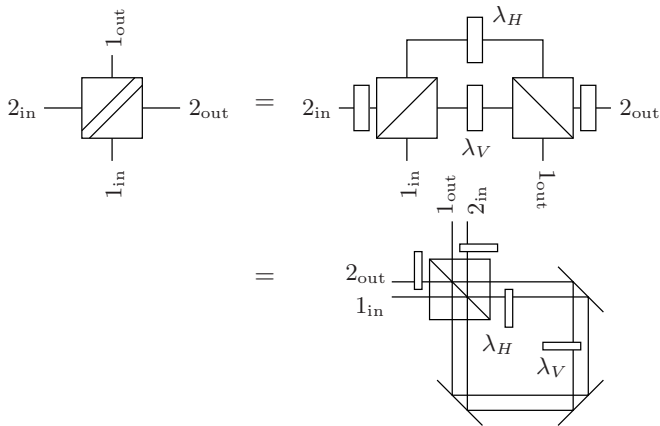


FIG. 4. From left to right: (i) A PPBS implementing a beam splitter with polarisation dependent reflectivity. (ii) It is equivalent to an interferometer between two PBS where the PPBS' reflectivities are incorporated by means of wave plates, λ_1 and λ_2 . (iii) By identifying the two PBS, the interferometer collapses into a closed loop (which is more compact and more robust in experimental implementations), leaving only one PBS. In the second and third circuit, a polarisation flip of the second qubit before and after the circuit is added by using a wave plate.

– tailored to the specific physical implementation at hand. Waveguide based setups would not need further simplifications because stability of the interferometers would be ensured by the rigid substrate. Implementations more suitable for beam displacer based setups are known [7]. Influenced by the gate model, those gates include a controlled π -phase gate at the core. Operating at lower success probabilities, especially at phases φ approaching 0, the probability of success does not converge to 1.

In the following we will discuss simplifications which shall allow for easier free-space implementation of the networks introduced above while still preserving optimality with respect to p_s . A straightforward set-up on dual-rail encoding that realises a three-mode unitary and compensates the amplitudes in the remaining modes is shown in Fig. 2. It includes one interferometer, but the whole gate would sit inside a double interferometer, because local unitaries on the input and output qubits would require classical interference. Thus, the complexity of this gate is best described as a nested three-fold interferometer. In this first stage, the parameters (reflectivities and phases) of all five beam splitters depend on φ .

To get rid of some of the interferometers, polarisation encoding is convenient. Two modes can be united in one spatial mode, resulting in inherent stability (neglecting birefringence of the optical medium) of some interferometers. Rotations on these modes can be carried out easily using wave plates. Because the core acts on modes coming from different dual-rail qubits, they have to be combined into a single spatial mode before. This is achieved with a PBS, thus permuting H and V modes. Damping of both by-passed modes can be done simultaneously by a single polarisation insensitive beam splitter coupled to the vacuum. A straightforward translation of Fig. 2 into polarisation encoding, thereby collapsing the net-

work into a single interferometer, is shown in Fig. 3.

Due to the asymmetry of the core, still one PPBS is used, the reflectivity of one polarisation component of which actually depends on φ , the other one being 1. Fig. 4 shows how a tunable PPBS can be constructed, introducing another interferometer.

Iterating the ideas that led to the compact PPBS implementation once more yields a collapsed form of the phase gate based on only two PBS and a couple of wave plates. Due to the paths of light being very similar, this set-up should also be more robust. This is illustrated by Fig. 5 since it has an overall Mach-Zehnder interferometer structure to it, by feeding one displaced sagnac loop into another.

E. Simple decomposition

Here we want to obtain a simple decomposition and explicit φ -dependence of the involved elements of the full 3×3 unitary transformation $U \in SU(3)$. To do so, we interpret the effective core, acting on the $|1\rangle_1$ and $|1\rangle_2$ modes in Fig. 2, in a different way: in between U_{λ_1} (the unitary beam splitter matrix of λ_1) and U_{λ_2} , there acts a diagonal mode transformation such that the first mode is unaffected and the amplitude of the second one is damped (due to U_{λ_V} coupling it with reflectivity r_V to a vacuum mode which will be projected onto the vacuum).

Now considering the singular value decomposition (SVD) of the matrix representing the core transformation, $A = V \cdot \Sigma \cdot W^\dagger$ we can identify $V = U_{\lambda_2}$, $W^\dagger = U_{\lambda_1}$ and $\Sigma = \text{diag}\{1, r_V\}$. As we have seen earlier, optimal extensions of 2×2 cores only require global rescaling, which commutes with the unitaries involved. Therefore we can use the much simpler original form of A in Eqn. (9), and we choose $x = 1$ and $y = -\sqrt{e^{i\varphi} - 1}$.

We find the singular values of A

$$\sigma_{\pm} = \sqrt{1 + 2 \sin \frac{\varphi}{2} \pm 2(2 - 2 \cos \varphi)^{1/4} \cos \frac{\varphi + \pi}{4}}. \quad (17)$$

Global rescaling amounts to fixing the largest singular value to unity, so the new singular values are 1 and $r_V = \sigma_- / \sigma_+$.

Due to $\det U_{\lambda_1} = \det U_{\lambda_2} = 1$ we need to attach a phase to one singular value as well in order to apply the identification of the matrices introduced above. Then the SVD of A yields

$$U_{\lambda_1} = \frac{1}{\sqrt{2}} \begin{bmatrix} -1 & 1 \\ -1 & -1 \end{bmatrix} \quad (18)$$

and $U_{\lambda_2} = U_{\lambda_1}^{-1} \cdot e^{i\phi_+ + \sigma_z}$ with

$$\phi_{\pm} = \text{arccot} \left[\cot \frac{\varphi + \pi}{4} \pm \left((2 - 2 \cos \varphi)^{1/4} \sin \frac{\varphi + \pi}{4} \right)^{-1} \right] \quad (19)$$

where the order of rows and columns in the matrices is as in Fig. 2 from top to bottom.

The ‘‘complex singular values’’ are 1 (the first mode is not affected) and $\sigma_- / \sigma_+ \exp i\phi_+ + \phi_-$. The latter can be

achieved by using the aforementioned coupling to the vacuum with a reflectivity of r_V and a phase upon reflection of $\phi_+ + \phi_-$. The further ingredients are the beam splitters required for the “damping” of the by-standers as discussed earlier. By confirming $1/\sigma_+^4 = p_s$ in the range $0 \leq \varphi \leq \pi$, the optimality of this construction is assured.

III. EVENT-READY GATES

Coming from post-selected gates, the next step towards scalable quantum computation would be to build gates not requiring measurements on the output modes. Intuitively it is clear that the construction of a controlled phase gate in this class will be more demanding with respect to the resources (such as the number of auxiliary modes and photons, size and complexity of the network) involved.

Especially the number of additional photons will change drastically: having had none in the post-selected case of a controlled π -phase gate, two are required in the class of event-ready gates. We will use this example as a motivation for a detour to discussing a number of different methods that could be useful for handling linear optics state preparation.

To do so, we notice that a controlled π -phase gate is more constrained than a device that creates EPR pairs from single photons. This is meant in the sense that it not only amounts to a state transformation from two single photons to an EPR pair, but a full unitary transformation on the entire computational state space in dual-rail encoding (and creating an EPR pair when applied to a certain product input corresponding to the product state of two photons). In the following two sections we will be concerned with different methods to describe linear optics state preparation and will apply them to the specific example at hand (i.e., heralded dual-rail EPR pair generations from single photons).

It will turn out, that the construction of an EPR pair out of single photons by means of linear optics, vacuum modes, one additional photon, and detectors is not possible. Of course, directly solving the polynomial equations in the matrix elements of A (generalisation of Eqns. (3) to (6)) will yield the same result – no solutions unless two additional photons are involved. Having excluded the cases of zero and one auxiliary photons, a set-up with two of them is possible, proven by the existence of such a scheme (EPR construction [22] as well as controlled- Z gate [1]).

A. State transformations

An obvious way of looking at states of exactly 2 photons in m bosonic field modes is the following. Such a state vector can be written as

$$\begin{aligned} |\psi_M\rangle &= P(\mathbf{a}^\dagger)|\text{vac}\rangle \\ &= \sum_{i,j=1}^m M_{i,j} a_i^\dagger a_j^\dagger |\text{vac}\rangle = (\mathbf{a}^\dagger)^T M \mathbf{a}^\dagger |\text{vac}\rangle, \end{aligned} \quad (20)$$

where M is a symmetric $m \times m$ matrix [?]. The application of a unitary mode-transformation U —representing a linear optical network—is reflected by

$$|\psi_M\rangle \mapsto |\psi_{M'}\rangle = (U \mathbf{a}^\dagger)^T M (U \mathbf{a}^\dagger) |\text{vac}\rangle \quad (21)$$

$$= (\mathbf{a}^\dagger)^T M' \mathbf{a}^\dagger |\text{vac}\rangle \quad (22)$$

with $M' = U^T M U$ clearly again being symmetric. As a special case of the singular value decomposition [23], a diagonal M' can be achieved, given an arbitrary input state vector $|\psi_M\rangle$.

Now let us choose U such that M' is diagonal. Then, labelled by

$$\nu' = \text{rank}(M'), \quad (23)$$

there are m different classes of states [16, 17], in each of which the states are composed by superpositions of 2 photons in either of ν' modes. These classes are separated by linear optical mode transformations requiring additional modes. Decreasing the rank is possible by allowing for auxiliary vacuum modes. However, to increase the rank by 1 one additional photon is required.

Further, the state matrix M of two single photons on four modes has rank $\nu = 2$ while an EPR pair corresponds to a matrix with rank $\nu = 4$. Therefore, the desired state transformation requires at least two additional single photons.

B. Polynomial factorisation

An alternative approach is the following [16]: The polynomial describing the objective state vector $|\psi\rangle = P(\mathbf{a}^\dagger)|\text{vac}\rangle$ with

$$P(\mathbf{a}^\dagger) = 2^{-1/2} \left(a_1^\dagger a_3^\dagger + a_2^\dagger a_4^\dagger \right) \quad (24)$$

does not factorise over \mathbb{C} . Using Lemmata 1 and 2 from Ref. [24], the property of factorisation of a bivariate polynomial

$$p(x, y) = \sum_{i,j=0}^m p_{i,j} x^i y^j \quad (25)$$

over \mathbb{C} can be tested by assessing the rank of a complex $2m(2m-1) \times (m+1)(2m-1)$ matrix. Further, applying Lemma 7 of Ref. [25], this technique can be extended to multi-variate polynomials. Now, a state can be constructed from a product state using linear optical gate arrays iff the corresponding polynomial is factorisable. In the case mentioned before (dual-rail EPR pair, so four variables), one can use the resulting 12×9 matrix to confirm in the language of polynomials of creation operators that additional resources are in fact required.

IV. TOFFOLI GATES

In the same way as above, we can consider a generalised Toffoli gate, the effect of which on the computational basis

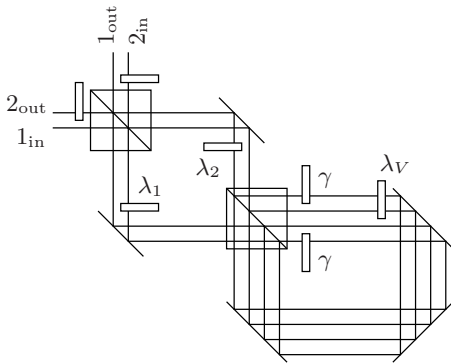


FIG. 5. Compact implementation of a controlled phase gate by using a single loop to implement the central PPBS and the compensation beam splitters simultaneously. Additionally, the two PBS are identified, resulting in a second loop. All omitted modes are initialised in the vacuum and post-selected in the vacuum state (which will be achieved in practice by counting the photons in the other output).

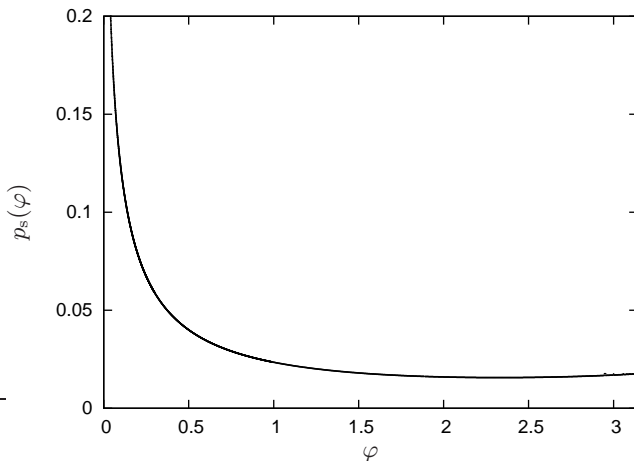


FIG. 6. Optimal success probabilities of generalised Toffoli gates. The features exhibited by $p_s(\varphi)$ are similar to the ones observed at the controlled phase gate (Fig. 1): There is a shallow dip between $\varphi = \pi/2$ and $\varphi = \pi$ below $p_s(\pi) = p_s(\pi/2)$ and a steep incline (more pronounced than for the controlled phase gate) for small phases towards $p_s(0) = 1$.

realized as dual-rail encodings can be described by the unitary

$$U = \text{diag}(1, 1, 1, 1, 1, 1, 1, e^{i\varphi}). \quad (26)$$

The solutions to the polynomial equations describing the action on the three-mode core—up to mode permutations—can be parametrised by $x, y \in \mathbb{R}$ and are given by the matrix

$$A = p_s^{1/6} \begin{bmatrix} 1 & \frac{e^{i\varphi}-1}{xy} & 0 \\ 0 & 1 & y \\ x & 0 & 1 \end{bmatrix}. \quad (27)$$

This has to be understood similar to the 2-mode core used by the controlled phase gate. However, here we do not solve the full optimisation problem, but only consider global rescaling.

For a unitary extension all singular values of A have to be at most 1. In order to avoid to formulate cubic singular values

explicitly, we use the following constraints. Let $p_{AA^\dagger}(\lambda) = \det(AA^\dagger - \lambda \mathbb{1}_3)$ be the characteristic polynomial of AA^\dagger , the roots $\lambda_{1,2,3}$ of which are the squared singular values of A . By requiring $p_{AA^\dagger}(1) = 0$, one of the singular values has to be 1. For the roots of p_{AA^\dagger} are real-valued and non-negative, the condition that all other singular values are not larger than 1 is equivalent with the condition that all derivatives of p_{AA^\dagger} have the same sign at $\lambda = 1$. More formally, this results in further constraints of the form

$$(-1)^\alpha p_{AA^\dagger}^{(k)}(1) = (-1)^\alpha \left. \frac{dp_{AA^\dagger}(\lambda)}{d\lambda} \right|_{\lambda=1} \geq 0 \quad (28)$$

for $1 \leq k < n$ where $\alpha = 0, 1$ is fixed by the condition of $k = n$. For $\varphi = \pi$ the optimal p_s compliant with these conditions is

$$p_s(\pi) = 1 + 3 \left(2^{1/3} - 2^{2/3} \right) \approx 1/57. \quad (29)$$

See Fig. 6 for the maximum success probability in the range $0 \leq \varphi \leq \pi$. The corresponding networks could be constructed in the same way as above. However, they would consist of 3-mode cores (an interferometer composed of three partially polarising beam splitters) inside separate interferometers for each of the 3 qubits. For free space experiments more appealing approaches for the specific choice of $\varphi = \pi$ are presented in Refs. [26, 27], but leading only to success probabilities of at most $1/72$.

V. REMARKS ON PROCESS TOMOGRAPHY

Process tomography amounts to characterizing (or sometimes certifying) an unknown physical process. In practice, the task is to identify that completely positive map that is closest to the data with respect to some meaningful figure of merit. To accomplish this task, one has to consider a tomographically complete set of inputs and look at Hilbert-Schmidt scalar products of the output with observables, to faithfully reconstruct the matrix form of the channel [30, 31]. Practically, the closest physical process can then be found by solving a convex optimization problem. Formally equivalently, and in instances in an experimentally simpler fashion, one can, instead of sending in a full set of input states, submit half of a single fixed maximally entangled state, and hence reconstruct the channel from the Choi matrix, then referred to as entanglement-assisted process tomography.

The latter technique can clearly also be applied in case of a postselected quantum gate like a phase gate. Yet, even without entangled inputs and including the actual measurement, one can reconstruct the resulting POVM elements, to which essentially postselected gates amount to when one faithfully includes also the actual measurement in the black-box description of the process. If one has a well-characterized source at hand, then the statistics of

$$p_{j,k} = \text{tr}[\rho_j A_k], \quad (30)$$

uniquely characterize the process, where $\{\rho_j\}$ form a tomographically complete well-characterized input set, and

$A_1, \dots, A_K \geq$ constitute a POVM, i.e.,

$$\sum_{k=1}^K A_k = \mathbb{1} \quad (31)$$

(for an experimental realization of such an approach, see Ref. [32]). In practice, one uses methods of convex optimization to identify the closest physical process to the given data.

For the purposes of the present work, one of the outcomes $k = 1$, that is, a specific pattern A_1 of detection, then gives rise to the actual postselected linear optical quantum gate. In this way, one can reconstruct postselected quantum gates, without using an ancilla-based approach, even faithfully including the final measurement as part of the process.

VI. CONCLUSION

We have shown how to obtain the maximum probability of success of controlled phase- and Toffoli-like gates in the

class of post-selected linear optics dual-rail gates without additional photons. Further, constructions of networks for the smaller gates suitable for experimental implementation have been given, and techniques elaborated upon that allow for the assessment of the possibility of certain linear optical schemes. For further progress concerning the eventual full optimization of linear optical processes it would be interesting to investigate (i) optimal constructions with respect to a class of gates inherently incorporating such experimental constraints or (ii) identify further decomposition techniques from a given linear optics mode transformation into suitable physical networks, respecting these constraints.

ACKNOWLEDGEMENTS

For insightful discussions concerning current experimental abilities we would like to thank M. Dušek, W. Wieczorek, C. Schmid, and J. Matthews. KK was supported by Microsoft Research through the European PhD Programme and the EU (MINOS), JE by the EU (QAP, COMPAS, MINOS) and the EURYI award.

-
- [1] E. Knill, R. Laflamme, and G. J. Milburn, *Nature* **409**, 46 (2001).
- [2] W. J. Munro, K. Nemoto, T. P. Spiller, S. D. Barrett, P. Kok, and R. G. Beausoleil, *J. Opt. B* **7**, S135 (2005); J. L. O'Brien, *Science* **318**, 1567 (2007); I. A. Walmsley, *Science* **319**, 1211 (2008); M. Aspelmeyer and J. Eisert, *Nature* **455**, 180 (2008).
- [3] A. Politi, M. J. Cryan, J. G. Rarity, S. Yu, J. L. O'Brien, *Science* **320**, 646 (2008); B. J. Smith, D. Kundys, N. Thomas-Peter, P. G. R. Smith, and I. A. Walmsley, arXiv:0905.2933.
- [4] H. F. Hofmann and S. Takeuchi, *Phys. Rev. A* **66**, 024308 (2002).
- [5] T. C. Ralph, N. K. Langford, T. B. Bell, and A. G. White, *Phys. Rev. A* **65**, 062324 (2002).
- [6] N. K. Langford, T. J. Weinhold, R. Prevedel, K. J. Resch, A. Gilchrist, J. L. O'Brien, G. J. Pryde, and A. G. White, *Phys. Rev. Lett.* **95**, 210504 (2005); N. Kiesel, C. Schmid, U. Weber, R. Ursin, and H. Weinfurter, *Phys. Rev. Lett.* **95**, 210505 (2005); R. Okamoto, H. F. Hofmann, S. Takeuchi, and K. Sasaki, *Phys. Rev. Lett.* **95**, 210505 (2005);
- [7] B. P. Lanyon, M. Barbieri, M. P. Almeida, T. Jennewein, T. C. Ralph, K. J. Resch, G. J. Pryde, J. L. O'Brien, A. Gilchrist, and A. G. White, *Nat. Phys.* **5**, 134 (2009).
- [8] J. Eisert, *Phys. Rev. Lett.* **95**, 040502 (2005); S. Scheel and N. Lütkenhaus, *New J. Phys.* **6**, 51 (2004).
- [9] D. Gross and J. Eisert, *Phys. Rev. Lett.* **98**, 220503 (2007).
- [10] R. Raussendorf and H. J. Briegel, *Phys. Rev. Lett.* **86**, 5188 (2001).
- [11] M. A. Nielsen and I. L. Chuang, *Quantum computation and quantum information* (Cambridge University Press, Cambridge, 2000).
- [12] J. Eisert, K. Jacobs, P. Papadopoulos, and M. B. Plenio, *Phys. Rev. A* **62**, 052317 (2000).
- [13] J. I. Cirac, W. Duer, B. Kraus, and M. Lewenstein, *Phys. Rev. Lett.* **86**, 544 (2001); D. W. Berry, *Phys. Rev. A* **75**, 032349 (2007).
- [14] D. B. Uskov, A. M. Smith, and L. Kaplan, arXiv:0908.2482.
- [15] N. M. VanMeter, P. Lougovski, D. B. Uskov, K. Kieling, J. Eisert, and J. P. Dowling, *Phys. Rev. A* **76**, 063808 (2007).
- [16] K. Kieling, PhD thesis (Imperial College London, 2008).
- [17] K. Kieling, Linear optics state transformations, in preparation.
- [18] T. Nagata, R. Okamoto, J. L. O'Brien, K. Sasaki, and S. Takeuchi, *Science* **316**, 726 (2007).
- [19] J. L. O'Brien, G. J. Pryde, A. G. White, T. C. Ralph, and D. Branning, *Nature* **426**, 264 (2003).
- [20] A. Politi, J. C. F. Matthews, and J. L. O'Brien, *Science* **325**, 1221 (2009).
- [21] B. J. Smith, D. Kundys, N. Thomas-Peter, P. G. R. Smith, and I. A. Walmsley, *Opt. Exp.* **17**, 13516 (2009); J. C. F. Matthews, A. Politi, A. Stefanov, and J. L. O'Brien, *Nat. Phot.* **3**, 346 (2009).
- [22] Q. Zhang, X.-H. Bao, C.-Y. Lu, X.-Q. Zhou, T. Yang, T. Rudolph, and J.-W. Pan, *Phys. Rev. A* **77**, 062316 (2008).
- [23] R. A. Horn and C. R. Johnson, *Matrix analysis* (Cambridge University Press, Cambridge, 1985).
- [24] W. Ruppert, *Journal of Number Theory* **77**, 62 (1999).
- [25] E. Kaltofen, *Journal of Computer and System Sciences* **50**, 274 (1995).
- [26] T. C. Ralph, K. J. Resch, and A. Gilchrist, *Phys. Rev. A* **75**, 022313 (2007).
- [27] J. Fiurášek, *Phys. Rev. A* **73**, 062313 (2006).
- [28] N. Lütkenhaus, J. Calsamiglia, and K.-A. Suominen, *Phys. Rev. A* **59**, 3295 (1999).
- [29] J. Calsamiglia, *Phys. Rev. A* **65**, 030301 (2002).
- [30] J. L. O'Brien, G. J. Pryde, A. Gilchrist, D. F. V. James, N. K. Langford, T. C. Ralph, and A. G. White, *Phys. Rev. Lett.* **93**, 080502 (2004).
- [31] A. Černoč, J. Soubusta, L. Bartušková, M. Dušek, and J. Fiurášek, *Phys. Rev. Lett.* **100**, 180501 (2008); W. Wieczorek, C. Schmid, N. Kiesel, R. Pohlner, O. Guehne, and H. Weinfurter, *Phys. Rev. Lett.* **101**, 010503 (2008).

- [32] J. S. Lundeen, A. Feito, H. Coldenstrodt-Ronge, K. L. Pregnell, Ch. Silberhorn, T. C. Ralph, J. Eisert, M. B. Plenio, and I. A. Walmsley, *Nat. Phys.* **5**, 27 (2009).